Food Chemistry: X 14 (2022) 100320

Contents lists available at ScienceDirect

Food Chemistry: X

journal homepage: www.sciencedirect.com/journal/food-chemistry-x

High-pressure processing influences the conformation, water distribution, and gel properties of pork myofibrillar proteins containing *Artemisia sphaerocephala* Krasch gum

Shengming Zhao [a,b,*], Zhao Li [a,b], Yu Liu [a,b], Yanan Zhao [a,b], Xiaorui Yuan [a,b], Zhuangli Kang [a,b], Mingming Zhu [a,b], Hanjun Ma [a,b]

[a] School of Food Science and Technology, Henan Institute of Science and Technology, No. 90 Hua lan Street, Xinxiang 453003, PR China
[b] National Pork Processing Technology Research and Development Professional Center, No. 90 Hua lan Street, Xinxiang 453003, PR China

ARTICLE INFO

Keywords:
High-pressure processing
Artemisia sphaerocephala Krasch gum
Protein conformation
Water distribution
Gel properties

ABSTRACT

The effect of high-pressure processing (100–4 00 MPa) on conformation, water distribution, and gel characteristics of reduced-sodium (0.3 M NaCl) myofibrillar protein containing 0.15% *Artemisia sphaerocephala* Krasch gum (AG) was investigated. The addition of AG resulted in the increase of WHC, proportion of immobilized water, and gel strength. Then, the WHC, proportion of immobilized water, and gel strength peaked after 200 MPa treatment, attributed to increased solubilization and zeta potential of MP, decreased particle size of MP, exposure of intrinsic tryptophan residues and the partial transformation of α-helix into β-sheet in MP. Moreover, 300 and 400 MPa induced decreases in surface hydrophobicity, solubility and storage modulus, resulting in the formation of loose and disordered gel structures with attenuated WHC. These results suggest that application of moderate HPP (200 MPa) combined with AG could provide a novel approach to improve the WHC and gelation properties of reduced-sodium meat products.

Introduction

Consumer demand for healthy foods has increased, along with a focus on developing low-salt meat products.However, salt, especially NaCl, is an essential ingredient in meat products as a flavoring agent and for producing the desired texture. Low salt would result in partial solubilization of proteins, which can cause poor texture and low water-binding capacity of meat products. Therefore, reducing the salt content presents a challenge for maintaining other desirable qualities. Polysaccharides, such as carrageenan, flaxseed gum, xanthan gum, and gellan gum, are used to improve meat protein functionality and gelling properties in emulsion-type meat products (Ye et al., 2019; Li et al., 2019; Pan, Feng, Sun, Chen, and Xu, 2016; Villamonte, Jury, Jung, & Lamballerie, 2015). *Artemisia sphaerocephala* Krasch gum (AG), a natural plant heteropolysaccharide with a crosslinked structure, has been used as a food additive to improve texture properties because of its excellent chemical thermal stability, high water retention, adhesion, and elasticity (Liang, Sun, Cao, Li, & Wang, 2018). However, there are only few reports on protein conformation and gelling properties of meat products by AG addition. Therefore, it is essential to study the effect of AG on gelling properties of myofibrillar protein.

Gelling properties of proteins are closely associated to the physicochemical properties of MPs, such as protein crosslinking, solubility, and conformation (Wang et al., 2020). High-pressure processing (HPP), one of various non-thermal processing technology, plays a vital part in compensating for changes in physicochemical properties of MPs caused by salt reduction and is widely used in low-salt meat production (Wang et al., 2021). HPP can affect protein denaturation, conformation, and solubilization by disrupting electrostatic interactions between proteins to improve their gel properties. HPP has received extensive attention from scientists in emulsion-type meat product processing (Guo, Li, Wang, & Zheng, 2019). Moreover, the pressure level is an important factor influencing protein functional properties. Low levels of HPP (≤300 MPa) can increase the solubilization and aggregation of MPs, and high levels of HPP (>300 MPa) can result in degradation of MPs and collapse of the gel network structure (Zhang, Yang, Zhou, Zhang, & Wang, 2017). Some previous studies suggested that the addition of polysaccharides combined with HPP treatments may improve water-

* Corresponding author at: School of Food Science and Technology, Henan Institute of Science and Technology, No. 90 Hua lan Street, Xinxiang 453003, PR China.
E-mail address: zhaoshengming2008@126.com (S. Zhao).

https://doi.org/10.1016/j.fochx.2022.100320
Received 17 January 2022; Received in revised form 10 April 2022; Accepted 27 April 2022
Available online 30 April 2022

holding capacity (WHC) and texture properties (Villamonte et al., 2015). However, to our knowledge, there has been very few reports regarding the mechanism of the gelling properties of reduced-sodium MP-AG by HPP.

Accordingly, the aim of the present study was to investigate the effects of high-pressure processing (100–400 MPa) on the conformation, water migration, and gelling properties of pork MPs containing AG at low salt concentrations (0.3 M NaCl). The changes in WHC, solubility, gel strength, surface hydrophobicity, particle size distribution (PSD), intrinsic fluorescence spectra, dynamic rheological measurements, water migration, FT-IR, and microstructure of different treated pork myofibrillar proteins were used to elucidate the mechanisms of thermal gelation for pressurized MP-AG under reduced salt conditions.

Material and methods

Materials

Ten kilogram-pork longissimus dorsi (landrace, 100 ± 5 kg, approximately six months old) were collected from the Gaojin group (Xin Xiang, China). The pork longissimus dorsi were stored at −80 °C. After thawing at 4 °C for 18 h, frozen pork was used for subsequent experiments. AG (purity 99%) was acquired from YHLO Chemical Industry, China.

Extraction of MP

Approximately 400 g thawed pork longissimus dorsi were cut into small pieces and homogenized with isolate buffer (0.1 M NaCl, 2 mM $MgCl_2$, 1 mM (EGTA), 10 mM KH_2PO_4/K_2HPO_4, pH 7.0) by a homogenizer (T25, IKA, Germany) at a speed of 12,000 rpm for 1 min. After centrifuging at 2000×g for 20 min, the crude myofibril pellets were resuspended in a standard extraction buffer (0.6 M NaCl, 3.38 mM Na_2HPO_4, 15 mM Na_2HPO_4, pH 7.5) and stirred for 24 h at 4 ℃. Then MP supernatant were obtained by centrifugation (1000×g, 20 min) and the concentration of MP was measured by the Biuret method. The final concentration of 60 mg/mL MP was adjusted using a buffer solution (pH 7.0) containing 0.3 M NaCl before testing.

HPP

First, 135 mg of AG (1.5 g/L relative to MP solution; Supplementary Fig. S1) and 60 mL MP solution (containing 900 mg MP) were stirred for 10 min to form a homogeneous solution. The vacuum-packed samples (30 mL) were treated with a series of pressure levels (0.1–400 MPa) for 10 min at 25 ± 1 °C using a high-pressure equipment (S-FL-850–9-W/FPG5620YHL, Stansted Fluid Power Ltd., Stansted, UK). MP samples without pressurization (0.1 MPa) were used as controls. Subsequently, the pressurized samples were transferred to a refrigerator (4 °C) overnight before testing solubility, number of reactive sulfhydryl groups, surface hydrophobicity, PSD, intrinsic fluorescence spectra, and dynamic rheology. Then, thermal treatment at 85 °C for 15 min was used for further gelation. Finally, they were immediately chilled to room temperature with a running water and refrigerated at 4 °C overnight for further gelling property analysis.

WHC analysis

Approximately 10 g of sample was weighed before (W_1) and after centrifugation at 8,000 g for 10 min at 4 °C (W_2). The WHC (%) of samples was observed through the following formula:

$$\text{WHC } (\%) = W_2/W_1 \times 100\%$$

Solubility analysis

After centrifugation (10,000×g, 20 min), protein suspensions (5 mg/mL, pH 6.0) with or without AG by HPP were used for solubility analysis (Zhang et al., 2017). The protein concentration was determined using a Bradford protein assay kit (Solarbio, Beijing, China) and BSA (Sigma-Aldrich) as the protein standard. Protein solubility was expressed as the percentage in comparison with that of protein concentration before centrifugation.

Surface hydrophobicity

A method described for bromophenol blue (BPB) binding was used to measure surface hydrophobicity (Wang et al., 2021). 1 mL MP solution (5 mg/mL) and 200 μL of 1 mg/mL BPB were agitated at 25 °C for 10 min. After centrifugation (2,000 × g, 20 min), the absorbance of the supernatant was measured at 595 nm to calculate the amount of bound BPB (μg) through the following formula:

$$\text{Bound BPB } (\mu g) = 200\ \mu g \times (A_{\text{control}} - A_{\text{sample}})/A_{\text{control}}$$

where A is the absorbance at 595 nm.

Reactive sulfhydryl group analysis

The number of reactive sulfhydryl groups was determined according to Ellman and Beverridge's method by molar extinction coefficient. 1.5 mL MP solutions (5 mg/mL) were dissolved with 10 mL Tris-glycine buffer solution (pH 8.0), and 50 μL Ellman reagent. The mixture was shaken vigorously and then stood (25 ℃) for 1 h. The absorbance of the supernatant was measured at 412 nm after centrifugation (12,000 × g, 5 min).

Particle size distribution and zeta potential

The particle size distribution and zeta potential of protein suspensions (1 mg/mL, pH 7.0) was measured by a Mastersizer 2000 (Malvern Instruments Ltd., Worcester shire, UK) (Wang et al., 2020). The mean particle size of MP particles was obtained by the auto-correlation function, and water was used as the dispersant.

Intrinsic fluorescence spectra

The fluorescence spectra of protein samples (1 mg/mL) were measured by a Cary Eclipse spectrofluorometer (Agilent Ltd., Kuala Lumpur, Malaysia). The excitation and emission wavelength were set at 295 nm and 300–400 nm, respectively.

Gel strength analysis

The gel strength of the cooked samples was evaluated using a TA.XT. plus texture analyzer with a P/0.5. The samples were analyzed for the following testing parameters: 2 mm/s test speed, 50% compression ratio and 5 g trigger.

Dynamic rheological analysis

The dynamic rheological measurements of the samples were measured using a dynamic rheometer (HAAKE MARS III rheometer, Thermo Scientific, Germany) in oscillatory mode. The storage modulus (G′ value) was evaluated by A 35 mm parallel plate (P35 TiL plate probe). The samples (approximately 3 g) were heated from 20 °C to 80 °C at temperature increments of 2 °C/min under 0.1 Hz oscillation frequency.

LF-NMR

The water migration of samples was analyzed by a NMR Analyzer (Model PQ001, Niumag Electric Corporation, Shanghai, China). Approximately 2 g of MP gels were placed into a 15 mm NMR glass tube and analyzed at 22.6 MHz resonance frequency at 32 ℃. The spin–spin relaxation time (T_2) and its corresponding water population (PT_2) were measured using the CPMG sequence with a τ-value of 350 μs.

Fourier transform infrared (FT-IR) spectroscopy

Frozen-dried powder samples were scanned 32 times using Fourier infrared spectrometer (TENSOR 27, BRUKER Co., Germany) in the wavelength range of 4000–400/cm-1, resolution 4 cm-1. The PeakFit software was used to analyze the change in the protein secondary structure by the deconvolution of the amide I band (1600–1700 cm^{-1}) (Han et al., 2019).

SEM

The gel samples were immobilized with 2.5% glutaraldehyde solution for 48 h, followed by dehydration with different volume gradients (50%, 70%, and 90%) of ethyl alcohol. The samples were then gold coated and analyzed the microstructure images of the samples were obtained under 1000× magnification by a scanning electron microscope (Quanta 200, FEI Corporation, Portland, USA) (Xue, Qian, Yuan, Xu, & Zhou, 2018).

Statistical analysis

Each treatment was repeated in triplicates, and five replications were measured. Data are expressed as mean ± standard deviation (SD). The experimental results were processed by SPSS software (version 20.0). Duncan's multiple range test was used for determining significant differences between least-square means ($P < 0.05$).

Results and discussion

WHC

The WHC of MP containing 0.15% (W/V) AG was higher than that of MP without AG (Fig. 1 A). These results could be explained that the polysaccharide network of AG has better WHC (Liang, et al., 2018). Moreover, the molecular interaction between AG and MP could induce more hydrogen bonds and hydrophobic interactions, which favors the physical entrapment of water, contributing to an increase in WHC (Jiang et al., 2020). Jia, Ma, and Hu (2020) reported that cooking loss of chickpea-wheat composite flour-based noodles was significantly decreased by adding 0.5% AG. Some previous investigations have also reported better water retention of meat products by polysaccharide addition (Chang & Chin, 2020; Petcharat & Benjakul, 2017). Thus, AG, as a natural polysaccharide, has strong water-binding capacity and is dispersed in the interstitial spaces of the pork MP network (Liang et al., 2018). The WHC of the samples first increased and then decreased with further HPP (100–400 MPa). With increasing pressure treatment, the 200 MPa treatment exhibited the maximum observed value (93.96%) of WHC. The higher levels of pressure treatments (300–400 MPa) resulted in a remarkable decrease in WHC ($P < 0.05$). This trend is generally

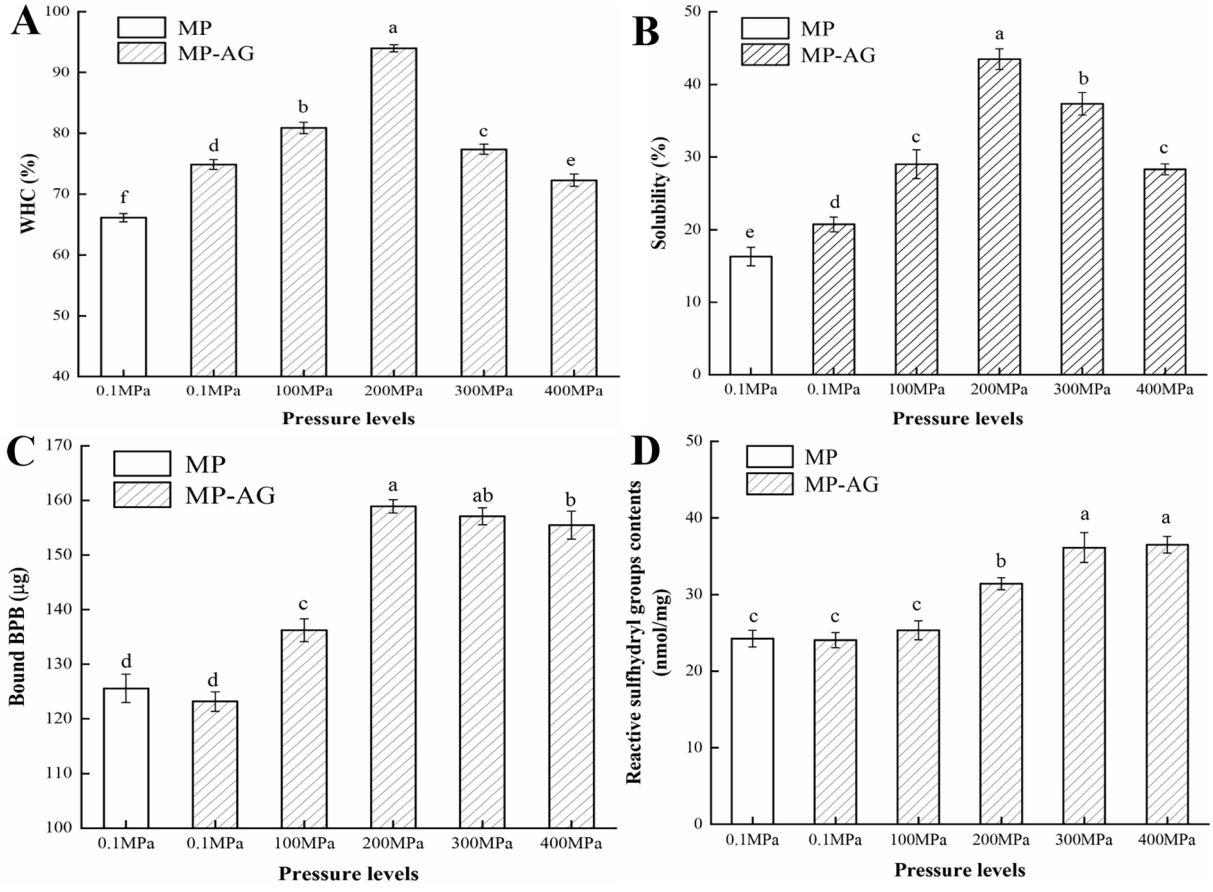

Fig. 1. Effects of HPP on the WHC (A) of MP-AG gels, solubility (B), surface hydrophobicity (C) and reactive sulfhydryl content (D) of MP-AG solutions. *a-f indicate significant differences on the histograms ($P < 0.05$).

similar with the study of Chen et al. (2010) that the WHC of duck muscle myosin was first increased and then decreased by HPP combined with curdlan. HPP can alter the structure of MP by increasing the charged groups of the amino acid residues, which promote the interactions between water and protein (Wang et al., 2020). Therefore, it was speculated that moderate HPP could promote hydrophobic interactions within the MP and AG addition, which contributed to the increase in the WHC of pressurized MP-AG gels. However, excessive pressure could collapse the gel network structure, resulting in water loss.

Solubility

The solubility of MP-AG compared with that of MP without AG was significantly enhanced ($P < 0.05$; Fig. 1 B). Previous studies have reported that the interactions between negative charge of xanthan gum and the partial positive charged groups of myofibrillar proteins could prevent the protein aggregation, resulted in the improvement of solubility (Villamonte et al., 2015). After HPP at 100–400 MPa, the solubility of MP-AG increased from 20.52% (0.1 MPa) to 29.23% (100 MPa) and reached a maximum value of 43.49% at 200 MPa. Degradation of MP was induced by HPP and then resulted in the formation of a short filament structure, which promotes the solubility of MP. Moreover, HPP induced MP exposing a more positively charged group, which interacted with the negative charge of AG for the formation of soluble complexes. The similar trend in solubility change of pork MPs reported by Villamonte et al. (2015), where the solubility of pork MPs containing xanthan gum was improved by 200 MPa treatment. Some previous studied have also indicated that HPP at 200 MPa could improve the solubility of soy protein and chicken MP (Manassero, Vaudagna, Anon, & Speroni, 2015). However, the solubility of MP-AG was significantly decreased ($P < 0.05$) by further increasing the pressure to 300 and 400 MPa. This could be explained by excessive pressure that induces MP denaturation by disrupting the tertiary structure (Marcos & Mullen, 2014). Wang et al. (2020) reported that 300 MPa treatment decreased the solubility of chicken MP and indicated that the solubility of MP is directly related to gelation properties. Our studies of WHC and gel strength are also consistent with the solubility (Fig. 1 A and Fig. 2 D). A moderate pressure level was found to improve the WHC and gel strength of MP-AG gels, which could be associated with increased protein solubility.

Surface hydrophobicity and reactive sulfhydryl groups

It has been recognized that surface hydrophobicity is essential in estimating the conformational modifications in protein structure (Wang et al., 2021). The bound BPB of MP was not changed by the incorporation of AG (Fig. 1 C), however the bound BPB of MP-AG significantly increased to 158.82 μg ($P < 0.05$) after 200 MPa pressure treatment. HPP induced protein unfolding for the formation of a destabilized conformation structure and resulted in the exposure of a greater number of hydrophobic sites. The increased hydrophobic residues could modify the tertiary structure of proteins significantly, inducing gelation of proteins. The study of Zhang et al. (2015) showed that the surface hydrophobicity of MP reached the maximum value at 200 MPa treatment. Conversely, the surface hydrophobicity of the protein decreased significantly ($P < 0.05$) when the pressure treatments reached 400 MPa. Excessive pressure induces an increase in aggregation between proteins

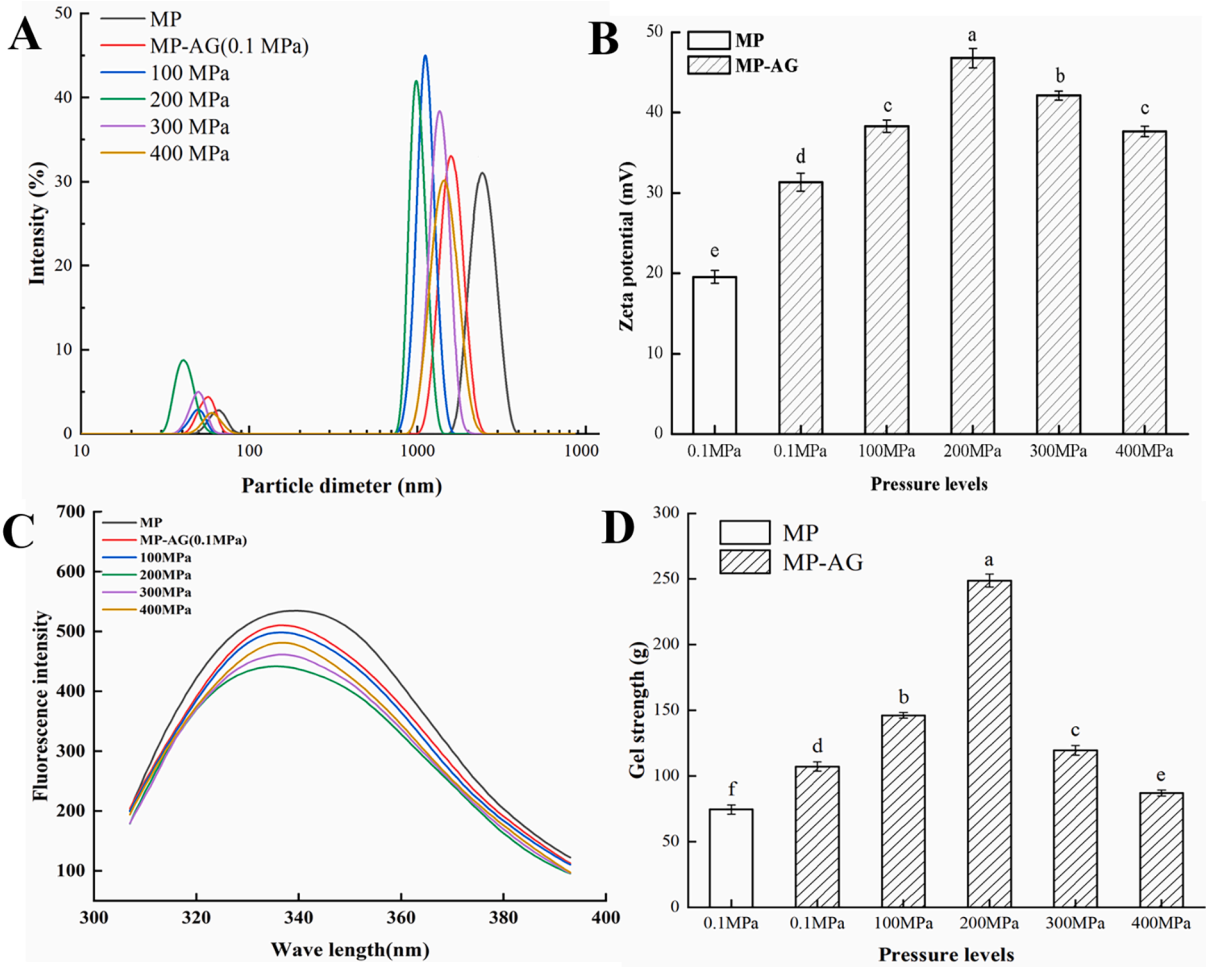

Fig. 2. Effects of HPP on the PSD images (A), zeta potential (B), intrinsic fluorescence spectroscopy (C) and gel strength (D) of MP-AG solutions.

that bury the exposed hydrophobic groups, resulting in a decrease in the surface hydrophobicity of MP (Zhang et al., 2016). The surface hydrophobicity is thought to be an important factor for MP aggregation, promoting the interaction between proteins and polysaccharides for gel formation. However, excessive exposure of hydrophobic groups may disperse the intermolecular forces, resulting in a decrease in WHC (Chen et al., 2014). It was previously reported that surface hydrophobicity had a negative influence on the protein solubility, the higher surface hydrophobicity and the lower solubility. Nevertheless, no similar results were found in the present study which probably because the particle size and zeta potential developed the greater impact in improving solubility rather than hydrophobicity (Wang, Jiang, Zhao, & Wang, 2020).

The sulfhydryl group, as an important determinant of protein functionality, is one of the most reactive forms of disulfide bonds under heating conditions (Zhang et al., 2015). The reactive sulfhydryl group content of MP was unchanged by the incorporation of AG (Fig. 1 D). However, the reactive sulfhydryl group content of MP-AG increased significantly ($P < 0.05$) with increasing pressure from 100 to 300 MPa. HPP induces protein denaturation and unfolding to expose sulfhydryl groups that are buried in the interior of the protein (Chan, Omana, & Betti, 2011). In the present study, with increases in pressure (100 to 300 MPa), further denaturation of MP resulted in greater exposure of active sulfhydryl groups. An insignificant increase ($P > 0.05$) in the sulfhydryl group content was observed after the pressure reaching to 400 MPa. Three hundred MPa was high enough to result in full exposure of the buried sulfhydryl groups. These results indicate that the active sulfhydryl groups are in line with the surface hydrophobicity (Fig. 1 C). Earlier studies also suggested that the improvement of surface hydrophobicity could be attributed to the increase in the content of active sulfhydryl groups by HPP (He et al., 2019). The molecular structure of MP is maintained prominently by disulfide bonds and hydrophobic interactions. Therefore, the increased surface hydrophobicity and active sulfhydryl group content indicated protein denaturation and unfolding.

PSD and zeta potential

The major peak of the PSD curve of the MP without AG was at approximately 2,895 nm (Fig. 2 A). The peak of MP with the incorporation of AG significantly shifted toward the smaller particle size region. The results were consistent with those of reports that the particle size of MP decreased with addition of flaxseed gum (Feng et al., 2018). The interaction of AG with MP induced a reduction in the electrostatic strength between molecules, resulting in a decrease in the mean particle diameter (Xu, Luo, Liu, & Mcclements, 2017). Then, HPP at 100 and 200 MPa elicited a shift in the major peak of the PSD curve of MP-AG toward a smaller particle size region (approximately 972 nm and 821 nm, respectively) which indicated that the particle size of MP-AG was decreased by low pressure treatment. Nevertheless, the shift of the major peak toward a larger size was obtained after pressure treatment from 300 to 400 MPa compared with that for samples treated by lower pressure. These results suggest that moderate pressure treatment (≤200 MPa) could contribute to MP degradation for the reduction of protein particle size. However, larger particles of MP-AG were observed under excessive pressure (>200 MPa), possibly because stronger HPP induced protein aggregation. The study of Hu et al. (2013) showed that the smaller the particle size, the better the WHC and strength of protein gels. Thus, the present results reveal that moderate HPP (≤200 MPa) could induce a smaller particle size of MP-AG which is conducive to improve gelation properties.

As shown in Fig. 2B, the negative zeta potential of MP-AG compared with that of MP without AG was significantly enhanced ($P < 0.05$) which probably because that AG, as a heteropolysaccharide containing anionic and neutral polysaccharides, could increase the negative charge of MP-AG, resulting in an increase in negative zeta potential value. Then, the negative potential value of MP-AG treated by HPP at 100 and 200 MPa were significantly increased ($P < 0.05$) and the peak value (45.52 mV) was observed by 200 MPa treatment. The weak electrostatic repulsion among untreated MP easily resulted in the formation of particle aggregate. However, moderate pressure treatment could induce partial unfolding of MP for the more exposure of charged amino acids at the protein surface, which facilitated the increase of absolute zeta potential value of MP (Zhu, Lanier, & Farkas, 2015). However, the absolute zeta potential of MP-AG was significantly decreased ($P < 0.05$) by further increasing the pressure to 300 and 400 MPa. This could be explained that stronger pressure level (>200 MPa) promoted the formation of protein aggregates through hydrophobic interaction, which expose less MP surface, resulting in the decreased in negative surface charge (Chen et al., 2016). Therefore, moderate pressure level could induce the MP-AG with high zeta potential, which can retard the formation of protein aggregates by interparticle electrostatic repulsions, contributing to the improvement in protein solubility (Fig. 1B).

Intrinsic fluorescence spectra

Trp fluorescence intensity of MP was significantly decreased by the incorporation of AG compared with that of MP without AG (Fig. 2 C). Trp residues are situated inside the hydrophobic environment of folded MPs, which results in higher fluorescence intensity (Cao & Xiong, 2015). However, Trp residues of unfolded MP are situated in a hydrophilic environment, resulting in a decrease in fluorescence intensity. Therefore, our results indicated that AG addition could interact with MP molecules for the tertiary structure unfolding of MP and expose more Trp residues in a hydrophilic environment. Thus, the Trp fluorescence intensity of the MP decreased. Jiang et al. (2020) reported that the incorporation of curdlan decreased the intrinsic fluorescence intensity of MP. The maximum fluorescence intensity of MP-AG was decreased after pressure treatment, indicating conformational changes in pressurized MP-AG. The maximum fluorescence intensity of MP-AG first decreased and then increased with the increasing pressure (100–400 MPa). The results of intrinsic Trp fluorescence spectra revealed that moderate pressure (≤200 MPa) promoted the exposure of more Trp residues in MP. High pressure levels (>200 MPa) could induce re-association of exposed hydrophobic Trp residues; thereafter, exposed tryptophan residues were buried. These results are in accord with the changes in surface hydrophobicity (Fig. 1 C). The exposure of hydrophobic amino acid from the interior of the proteins could alter the surface charge distribution and content of proteins, contributing to MP thermal gelation and finally improves the WHC (Fig. 1 A) and strength (Fig. 2 D) of MP-AG gels (Xue et al., 2017).

Gel strength

MP gel with AG was stronger than that of MP gel without AG (Fig. 2 D). AG, as a polymer, could increase gel strength of MP-AG gels by interacting with MP and forming a three-dimensional structure. Lee and Chin (2020) reported that the incorporation of basil seed gum resulted in higher gel strength of MP gels. Then, the MP-AG gels showed a trend of increasing first and then decreasing with the increasing pressure from 100 to 400 MPa. A high gel strength (248.88 g) was obtained when the samples were pressurized at 200 MPa. Moreover, after stronger HPP (300 and 400 MPa), the gel strength of the samples exhibited a remarkable decrease ($P < 0.05$). Similar results were observed at 100–500 MPa in surimi gels containing 0.8% (w/w) of κ-carrageenan (Ye et al., 2019). This might be because mild HPP could induce MP denaturation and stretch properly, resulting in the exposure of more hydrophobic groups of MPs. The exposed hydrophobic residues cross-linked to aggregate and sulfhydryl groups formed disulfide bonds for the formation of an intense gel network after heat-induced gelation (Zhang et al., 2017). In addition, more positively charged groups were exposed by HPP, which promoted the interactions of MP with AG for the formation of dense three-dimensional gel structures (Chen et al., 2014). A previous study on heat-induced chicken breast actomyosin gel also

indicated that the gel strength of actomyosin gel containing 0.5% (w/v) sodium alginate were significantly improved by 200 MPa treatment. However, a stronger pressure (>200 MPa) could result in the degradation or depolymerization of MPs, which induces a heterogeneous gel structure (Chen et al., 2014). Thus, a weakened gel strength of the samples was obtained. Zhang et al. (2017) found that moderate pressure treatment (≤200 MPa) strengthened the gel strength of MP gels, but stronger pressure treatment (>300 MPa) weakened the gel strength of MP gels. Therefore, it is speculated that the HPP-induced increase in gel strength of the pork MP containing AG was related to the interaction between meat protein and polysaccharide.

Dynamic rheology

The storage modulus (G') representing the elastic portion were used to describe the protein functionality (Zhang et al., 2017). As illustrated in Fig. 3 A, The G'of MP samples without AG exhibited two peaks heating from 20 °C to 80 °C. The first in the G' curve was observed at 48.5 °C, where myosin head and hinge portions were denatured and aggregated, contributing the formation of a loose gel structure. Then, G′ remarkably increased during the range from 20 °C to 80 °C, which referred to the further unfolding and aggregation of myosin for the formation of a cross-linked and more compact network structure (Chen et al., 2014). Incorporation of AG significantly increased the G' value of MP gels, indicating that the interaction between AG and MP during thermal gelation could promote the unfolding of myosin and actin chains before their orderly aggregation, resulting in a dense gel network formation and improve the elastic character of MP gels (Feng et al., 2018). The present results showed that there were no significant effects ($P > 0.05$) on surface hydrophobicity and reactive sulfhydryl groups between MP with and without AG (Fig. 1 C and 1 D); however, incorporation of AG resulted a higher G' (Fig. 3A), WHC (Fig. 1 A), and gel strength (Fig. 2 D) of MP gels during heating. The similar results are reported by Chen et al. (2014) who indicated that exposure of electriferous groups of MPs by unfolding and denaturation and interaction with anionic AG enhanced the elastic characteristic (G') of MP gel during heating. Thus, it could be explained that thermal treatment promoted the interaction between AG and MP to improve the gel properties of MP-AG gels.

Then, HPP treatment increased the G' of MP gels under 100 MPa and exhibited a significant decrease from 200 to 400 MPa. The results revealed that moderate HPP treatment accelerated the interaction between AG and MP under thermal gelation. However, high pressure levels (>200 MPa) resulted in a significant decrease in the G' value of MP-AG ($P < 0.05$), and the disappearance of the denaturation peak at 48 °C, which probably because the severe denaturation and aggregation of MP and induced by HPP treatment (Cando, Herranz, Javier Borderias, & Moreno, 2015). Thermal gelation is due to protein denaturation and crosslinking to form a continuous network structure. However, excessive HPP could accelerate protein denaturation and aggregation, leading to protein aggregation prior to heating for gelation, and fewer native protein molecules denatured to gelation, which would decrease the G' of MP (Sun & Holley, 2011). In the present study, HPP-induced protein-AG aggregation or protein–protein, might result in a low gelling ability. Meanwhile, the stronger pressure treatment (>200 MPa) induced the disappearance of dramatic decrease stage in the G' curve, which might be related to the increased surface hydrophobicity and sulfhydryl group content (Fig. 1 C and 1 D).

Low-field NMR measurements

Low-field NMR proton spin–spin relaxation time (T_2) is generally used to assess the distribution state of water in different samples. The LF-NMR T_2 relaxation curves and their populations (P_2) on the MP-AG gels are shown in Table 1 and Fig. 3 B. Fig. 5 shows that three relaxation populations were mostly located at 0–10 ms (T_{2b}), 50–600 ms (T_{21}), and 1000–5000 ms (T_{22}). T_{2b} bound water with shorter relaxation times and was tightly bound to other macromolecular constituents (Li et al., 2019). T_{21} (immobilized water) was the major component that represented water that was loosely trapped in the network structure of the MP-AG gels. T_{22} is free water located between fiber bundles as well as intermyofibrillar water (Yang, Han, Yun, Han, & Zhou, 2015). As illustrated in Table 1, T21 was significantly ($P < 0.05$) decreased by the addition, which indicating the decreased water mobility of the immobilized water. Moreover, compared with that for MP without AG, a significant increase in P_{21} (population of main immobilized water) from 80.74% to 86.86% and decrease in P_{22} (population of free water) from 18.59% to 12.36% ($P < 0.05$) of MP-AG samples was observed. Therefore, it can be inferred that AG could increase the proportion of water tightly bound to the gel network. HPP from 100 to 400 MPa shifted the positions of T_{2b}, T_{21}, and T_{22} of MP-AG gels toward lower relaxation times (Fig. 3B). It is noteworthy that 200 MPa exhibited the shortest relaxation time, which indicates that 200 MPa significantly weakened water mobility. Moreover, compared with that for unpressurized samples, P_{2b} and P_{21} were significantly increased and P_{22} was significantly decreased at 200 MPa ($P < 0.05$) (Table 1). These results indicate that

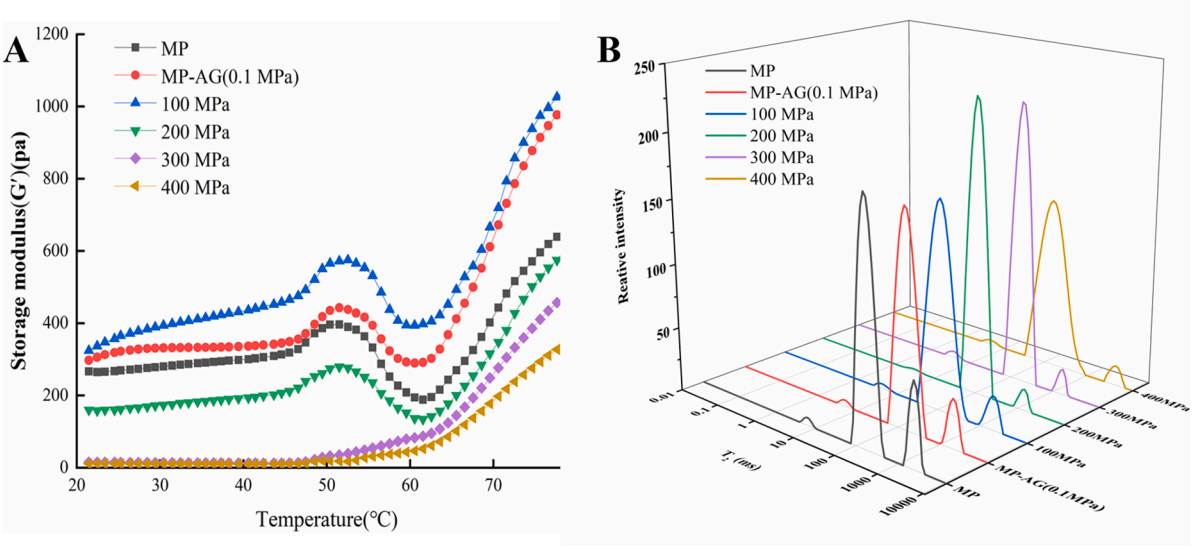

Fig. 3. Effects of HPP on the G' (A) and distribution of T_2 relaxation times (B) of MP-AG gels. *a-f indicate significant differences on the histograms ($P < 0.05$).

Table 1
Effects of HPP on low-field NMR relaxometry T_2 relation times and relaxometry proportions of peak areas of MP-AG gels.

Sample	Initial relaxation time/ms			Peak ration/%		
	T_{2b}	T_{21}	T_{22}	P_{2b}	P_{21}	P_{22}
MP	1.74 ± 0.58^{a}	69.08 ± 5.69^{a}	1429.27 ± 53.30^{a}	1.12 ± 0.10^{b}	80.74 ± 0.32^{e}	18.59 ± 0.47^{a}
MP-AG (0.1 MPa)	1.18 ± 0.36^{b}	57.62 ± 2.20^{b}	1385.93 ± 32.34^{ab}	1.44 ± 0.03^{a}	86.60 ± 1.04^{d}	12.36 ± 1.05^{b}
100 MPa	0.70 ± 0.24^{bc}	50.59 ± 6.27^{bc}	1245.91 ± 80.96^{c}	1.14 ± 0.10^{b}	91.99 ± 0.80^{c}	7.09 ± 0.27^{c}
200 MPa	0.32 ± 0.01^{c}	43.10 ± 2.01^{c}	1049.96 ± 59.43^{d}	1.50 ± 0.07^{a}	95.44 ± 0.34^{a}	3.78 ± 0.24^{e}
300 MPa	0.48 ± 0.17^{c}	50.58 ± 6.03^{bc}	1237.90 ± 87.69^{c}	1.35 ± 0.14^{a}	94.34 ± 0.12^{ab}	4.21 ± 0.07^{de}
400 MPa	0.75 ± 0.12^{bc}	58.60 ± 6.61^{b}	1281.15 ± 41.92^{bc}	1.13 ± 0.03^{b}	94.16 ± 0.72^{b}	4.77 ± 0.32^{d}

*a-f indicate significant differences on the histograms ($P < 0.05$).

HPP could be conductive to the transition from free water to immobilized water. Some studies have suggested that protein aggregation and gel formation under HPP coul induce the reduction of the relaxation time of water protons. Another possible explanation for this is that HPP treatment can promote intermolecular hydrogen bond formation within the waters and the protein-polysaccharide matrix to alter the T_2 value (Han et al., 2019). Ye et al. (2019) found that HPP was able to increase WHC in surmi-carrageenan gels by significantly lowering its water mobility. Hence, these results indicate that increasing P_{21} and decreasing P_{22} using AG and HPP could contribute to a higher WHC of the MP-AG gel.

FT-IR

As shown in Fig. 4, the spectral types of FTIR of all samples were exhibited the similar patterns. The amide A band (3000–3500 cm^{-1}, N—H or O—H stretching) was usually used to assess the interaction between water molecules and protein. Compared with the MP without AG (amide A band at 3305.4 cm^{-1}), MP-AG gel observed the lower wave number of amide A band at 3299.6 cm^{-1}, indicating that the incorporation of AG promoted hydrogen bond formation within MP-AG (Chen et al., 2014). Then, with the increase HPP treatment pressure (100–400 MPa), the significantly red-shifted peaks of the amide A band in MP-AG gels was found at 3295.7 cm^{-1},3288.2 cm^{-1}, 3297.3 cm^{-1}, 3301.6 cm^{-1}, respectively. This phenomenon could be explained that moderate pressure treatment could improve the intermolecular hydrogen bonds, resulting in an increase in WHC and the gel strength. The similar trend in HPP treated surimi gels containing κ-carrageenan was reported by Ye et al. (2019).

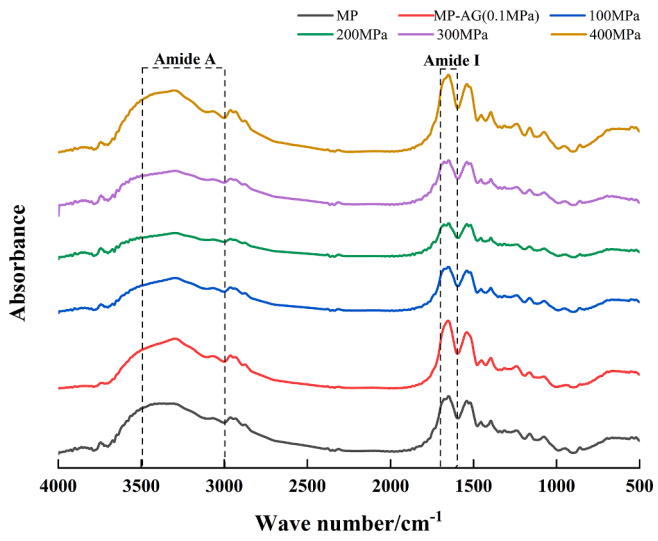

Fig. 4. Effects of HPP on FTIR spectra of MP-AG gels.

The amide I band (C═O and C═N stretching) between 1600 and 1700 cm^{-1} was commonly used to calculated the proportions of protein secondary structure. The proportions of α-helix, β-sheet, β-turn and random coil were illustrated in Table 2. The incorporation of AG showed lower α-helix and β-turn contents and higher β-sheet were higher than that of the MP gels without AG ($P < 0.05$). The random coil of MP was not significantly influenced by AG addition ($P > 0.05$). The loss of a-helix structures and the formation of β-sheet were generally considered to the result of protein unfolding. Thus, the interaction between MP and AG promoted the unfolding of MP, contributing to the modification of protein secondary structure (Villamonte et al., 2015). With increasing pressure treatment, the α-helix and β-turn contents decreased and then increased, and reached minimum value at 200 MPa (28.29% and 8.39%, respectively). The contents of β-sheets and random coil significantly increased as the increased pressure treatment. The 200 MPa treatment exhibited the peak value (45.74%) of β-sheet. The probably explanation is that the partial unfolding of the helical structures in MP induced by interaction between MP and AG under HPP treatment resulted a transition from α-helix to β-sheet structures (Zhang et al., 2017). Moreover, the exposure of hydrophobic groups (Fig. 1 C) the sulfhydryl group (Fig. 1 D) and of the MP induced by HPP also contributed to the loss in the α-helix and increase in the β-sheet content. Accordingly, HPP could induce the unfolding of MP and exposure of hydrophobic residues, resulted in a change of protein secondary structure for the stable three-dimensional network with high WHC.

Microstructure

The microstructure of the MP-AG gel was highly associated with its texture and WHC. As illustrated in Fig. 5, a gel network with disordered cavities, rough crosslinking chains, and a scattered structure of unpressurized MP gels were observed. The rapid water loss during heating for the formation of disordered cavities inside the tissue could explain this phenomenon. Moreover, there was a dense structure with small and well-distributed cavities in unpressurized gels with the addition of AG. This result signified that AG as a polysaccharide might fill in the cavities of the protein space, resulting in the formation of a smooth, compact, and uniform gel matrix. These results are consistent with the reports by Li et al. (2019), who showed that the incorporation of 1% curdlan induced the formation of a denser gel structure. Thus, the structure facilitated the entrapment of water for a higher WHC (Fig. 1 A). Compared with unpressurized samples, after HPP under 200 MPa, MP-AG gels exhibited a denser and more homogeneous network containing numerous small cavities because the protein began to unfold. This could be attributed to the fact that MPs had the smallest particle size at 200 MPa, which was conducive to the formation of a dense network (Fig. 2 A). Moreover, more exposure to hydrophobic residues (Fig. 1 C) also benefited the formation of a uniform network. However, with excessive pressure treatment (≥300 MPa), a crumb-like network structure with large and heterogeneous cavities was formed which could be responsible for the low water-binding capacity (Fig. 1A). The results could be explained by the higher pressure inducing denaturation and aggregation of MPs that occurred faster than unfolding speed, thus protein segments aggregated easily to form globular aggregates and an irregular network during thermal gelation. Similar results were also observed for the effects of different pressures (100–500 MPa) on chicken breast MP gels (Zhang et al., 2017). Chen et al. (2014) also reported similar microstructure observations of chicken breast actomyosin gel

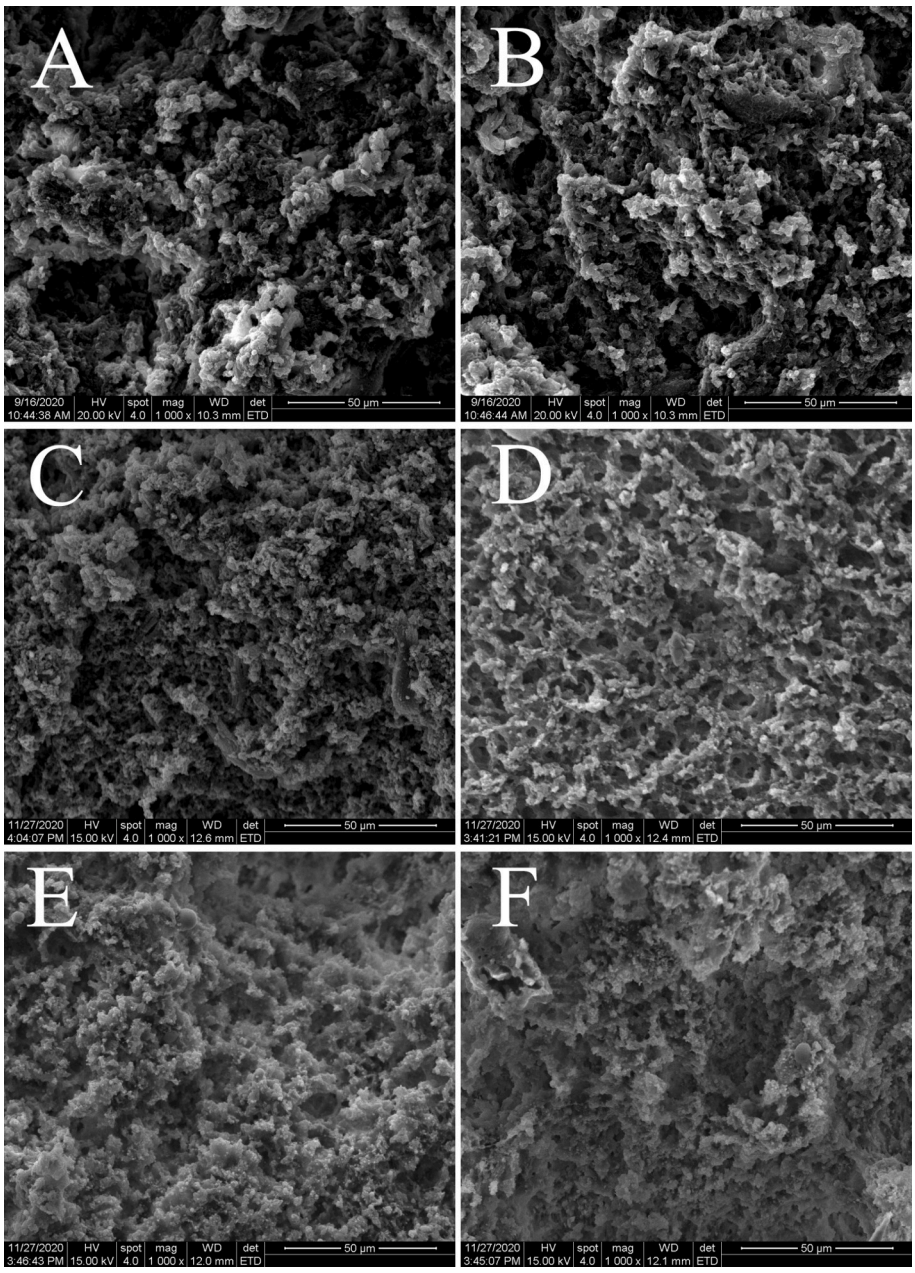

Fig. 5. SEM microstructure of MP-AG gels by HPP at 1000 × (A-F). (A) MP 0.1 MPa, (B) MP-AG 0.1 MPa, (C) MP-AG 100 MPa, (D) MP-AG 200 MPa, (E) MP-AG 300 MPa, (F) MP-AG 400 MPa.

after pressure treatment (100–400 MPa).

Conclusions

This paper shows that adding AG increased both the WHC and gel strength. HPP at 100–200 MPa further improved the WHC and gelation properties of MP-AG gel, as evidenced by the increasing immobilized water content, reduced particle size, and increasing zeta potential of MP, the increasing exposure of Trp residues, and the formation of a dense and homogeneous gel network. FTIR showed that addition of AG and 100–200 MPa pressure treatment significantly decreased the α-helix content and β-sheet content. However, excessive HPP (300 and 400 MPa) could contribute to the attenuated solubilization of MP which was attributed to the enhanced reactive sulfhydryl group content and zeta potential, the reduced surface hydrophobicity, and reduced exposure of Trp residues. Moreover, strong pressure induced an increase in particle size for the formation of protein aggregates and the formation of a crumb-like network structure of the MP-AG gel. Overall, the HPP level of 200 MPa combined with AG inducing the formation of a dense and homogeneous gel network with high WHC and gel strength could be considered as a promising approach for the improvement in quality attributes of reduced-sodium gel-type meat products.

CRediT authorship contribution statement

Shengming Zhao: Funding acquisition, Writing – original draft, Revision. **Zhao Li:** Methodology, Software. **Yu Liu:** Revision. **Yanan Zhao:** Data curation, Visualization. **Xiaorui Yuan:** Methodology. **Zhuangli Kang:** Investigation, Conceptualization. **Mingming Zhu:** Data curation. **Hanjun Ma:** Funding acquisition, Resources, Writing – review & editing.

Table 2
Effects of HPP on percentages of secondary structural components of MP-AG gels.

Sample	α-Helix (%)	β-Sheet (%)	β-Turn (%)	Random coil (%)
MP	32.34 ± 0.12[a]	35.76 ± 0.27[d]	16.50 ± 0.04[a]	15.9 ± 0.14[c]
MP-AG (0.1 MPa)	31.26 ± 0.63[b]	39.31 ± 0.25[c]	13.99 ± 0.84[b]	15.47 ± 0.36[c]
100 MPa	29.19 ± 0.25[c]	43.98 ± 0.16[b]	9.59 ± 0.23[c]	16.07 ± 0.14[a]
200 MPa	28.29 ± 0.17[d]	45.74 ± 0.43[a]	8.39 ± 0.49[d]	17.38 ± 0.16[b]
300 MPa	28.61 ± 0.18[d]	46.18 ± 0.92[a]	9.22 ± 0.18[c]	16.87 ± 0.18[b]
400 MPa	30.54 ± 0.32[b]	45.92 ± 0.26[a]	9.77 ± 0.34[c]	16.52 ± 0.32[b]

Note: Different letters of the same column indicate significant differences between groups ($P < 0.05$).

Declaration of Competing Interest

The authors declare that they have no known competing financial interests or personal relationships that could have appeared to influence the work reported in this paper.

Acknowledgment

This study was financially support by Key scientific and technological projects in Henan Province of China (grant no. 202102110060).

Appendix A. Supplementary data

Supplementary data to this article can be found online at https://doi.org/10.1016/j.fochx.2022.100320.

References

Cando, D., Herranz, B., Javier Borderias, A., & Moreno, H. (2015). Effect of high pressure on reduced sodium chloride surimi gels. *Food Hydrocolloids, 51*(10), 176–187. https://doi.org/10.1016/j.foodhyd.2015.05.016

Cao, Y., & Xiong, Y. (2015). Chlorogenic acid-mediated gel formation of oxidatively stressed myofibrillar protein. *Food Chemistry,* 2015, 180(8): 235-243. 10.1016/j.foodchem.2015.02.036.

Chan, J., Omana, D., & Betti, M. (2011). Application of high pressure processing to improve the functional properties of pale, soft, and exudative (PSE)-like turkey meat. *Innovative Food Science and Emerging Technologies, 12*(3), 216–225. https://doi.org/10.1016/j.ifset.2011.03.004

Chang, H., & Chin, K. (2020). Physical properties and structural changes of myofibrillar protein gels prepared with basil seed gum at different salt levels and application to sausages. *Foods, 9*(6), 702. https://doi.org/10.3390/foods9060702

Chen, X., Chen, C., Zhou, Y., Li, P., Ma, F., Nishiumi, T., et al. (2014). Effects of high pressure processing on the thermal gelling properties of chicken breast myosin containing κ-carrageenan. *Food Hydrocolloids, 40*(10), 262–272. https://doi.org/10.1016/j.foodhyd.2014.03.018

Chen C., Wang R., Sun G., Fang H., Ma D., & Yi S. Effects of high pressure level and holding time on properties of duck muscle gels containing 1% curdlan (2010). *Innovative Food Science & Emerging Technologies,* 11(4):538-542. 10.1016/j.ifset.2010.05.004.

Chen, X., Li, P., Nishiumi, T., Takumi, H., Suzuki, A., & Chen, C. (2014). Effects of high-pressure processing on the cooking loss and gel strength of chicken breast actomyosin containing sodium alginate. *Food and Bioprocess Technology, 7*(12), 3608–3617. https://doi.org/10.1007/s11947-014-1368-9

Chen, X., Xu, X., Han, M., Zhou, G., Chen, C., & Li, P. (2016). Conformational change induced by high-pressure homogenization inhibit myosin filament formation in low ionic strength solutions. *Food Research International, 85*(6), 1–9. https://doi.org/10.1016/j.foodres.2016.04.011

Feng, M., Pan, L., Yang, X., Xu, X., & Zhou, G. (2018). Thermal gelling properties and mechanism of porcine myofibrillar protein containing flaxseed gum at different NaCl concentrations. *LWT- Food Science and Technology, 87*(9), 361–367. https://doi.org/10.1016/j.lwt.2017.09.009

Guo, Z., Li, Z., Wang, J., & Zheng, B. (2019). Gelation properties and thermal gelling mechanism of golden threadfin bream myosin containing $CaCl_2$ induced by high pressure processing. *Food Hydrocolloids, 95*(10), 43–52. https://doi.org/10.1016/j.foodhyd.2019.04.017

Han, Z., Zhang, J., Zheng, J., Li, X., & Shao, J. (2019). The study of protein conformation and hydration characteristics of meat batters at various phase transition temperatures combined with low-field nuclear magnetic resonance and Fourier transform infrared spectroscopy. *Food Chemistry, 280*(5), 263–269. https://doi.org/10.1016/j.foodchem.2018.12.071

He, D., Wang, X., Ai, M., Kong, Y., Fu, L., Zheng, B., et al. (2019). Molecular mechanism of high-pressure processing for improving the quality of low-salt eucheuma spinosum chicken breast batters. *Poultry Science, 98*(6), 2670–2678. https://doi.org/10.3382/ps/pez027

Hu, H., Fan, X., Zhou, Z., Xu, X., Fan, G., Wang, L., et al. (2013). Acid-induced gelation behavior of soybean protein isolate with high intensity ultrasonic pre-treatments. *Ultrasonic Sonochemistry, 20*(1), 187–195. https://doi.org/10.1016/j.ultsonch.2012.07.011

Jia, F., Ma, Z., & Hu, X. (2020). Controlling dough rheology and structural characteristics of chickpea-wheat composite flour-based noodles with different levels of artemisia sphaerocephala krasch. gum addition. *International Journal of Biological Macromolecules, 150*(5), 605–616. https://doi.org/10.1016/j.ijbiomac.2020.02.101

Jiang, S., Zhao, S., Jia, X., Wang, H., Zhang, H., Liu, Q., et al. (2020). Thermal gelling properties and structural properties of myofibrillar protein including thermo-reversible and thermo-irreversible curdlan gels. *Food Chemistry*, 311(5): 126018.1-126018.8. 10.1016/j.foodchem.2019.126018.

Lee, C., & Chin, K. (2020). Physical properties and structural changes of myofibrillar protein gels prepared with basil seed gum at different salt levels and application to sausages. *Foods, 9*(6), 702. https://doi.org/10.3390/foods9060702

Li, K., Liu, J., Fu, L., Li, W., Zhao, Y., Bai, Y., et al. (2019). Effect of gellan gum on functional properties of low-fat chicken meat batters. *Journal of Texture Studies, 50*(2), 131–138. https://doi.org/10.1111/jtxs.12379

Li, Q., Wang, P., Miao, S., & Zhang, L. (2019). Curdlan enhances the structure of myosin gel model. *Food Science and Nutrition, 7*(6), 2123–2130. https://doi.org/10.1002/fsn3.1055

Liang, T., Sun, G., Cao, L., Li, J., & Wang, L. (2018). Rheological behavior of film-forming solutions and film properties from artemisia sphaerocephala krasch. gum and purple onion peel extract. *Food Hydrocolloids, 82*(9), 124–134. https://doi.org/10.1016/j.foodhyd.2018.03.055

Manassero, C., Vaudagna, S., Anon, M., & Speroni, F. (2015). High hydrostatic pressure improves protein solubility and dispersion stability of mineral-added soybean protein isolate. *Food Hydrocolloids, 43*(1), 629–635. https://doi.org/10.1016/j.foodhyd.2014.07.020

Marcos, B., & Mullen, M. (2014). High pressure induced changes in beef muscle proteome: Correlation with quality parameters. *Meat Science, 97*(1), 11–20. https://doi.org/10.1016/j.meatsci.2013.12.008

Pan, L., Feng, M., Sun, J., Chen, X., & Xu, X. (2016). Thermal gelling properties and mechanism of porcine myofibrillar protein containing flaxseed gum at various pH values. *CyTA-Journal of Food, 14*(4), 547–554. https://doi.org/10.1080/19476337.2016.1172261

Petcharat, T., & Benjakul, S. (2017). Effect of gellan incorporation on gel properties of bigeye snapper surimi. *Food Hydrocolloids, 77*(4), 746–753. https://doi.org/10.1016/j.foodhyd.2017.11.016

Sun, X., & Holley, R. (2011). Factors influencing gel formation by myofibrillar proteins in muscle foods. *Comprehensive Reviews in Food Science and Food Safety, 10*(1), 33–51. https://doi.org/10.1111/j.1541-4337.2010.00137.x

Villamonte, G., Jury, V., Jung, S., & Lamballerie, M. (2015). Influence of xanthan gum on the structural characteristics of myofibrillar proteins treated by high pressure. *Journal of Food Science, 80*(3), 522–531. https://doi.org/10.1111/1750-3841.12789

Wang, Y., Zhou, Y., Wang, X., Ma, F., Xu, B., Li, P., et al. (2020). Origin of high-pressure induced changes in the properties of reduced-sodium chicken myofibrillar protein gels containing $CaCl_2$: Physicochemical and molecular modification perspectives. *Food Chemistry, 319*(7), Article 126535. https://doi.org/10.1016/j.foodchem.2020.126535

Wang, Y., Jiang, S., Zhao, Y., & Zeng, M. (2020). Physicochemical and rheological changes of oyster (*Crassostrea gigas*) protein affected by high-pressure homogenization. *LWT - Food Science and Technology, 134*(3), Article 110143. https://doi.org/10.1016/j.lwt.2020.110143

Xu, X., Luo, L., Liu, C., & Mcclememts, D. (2017). Utilization of anionic polysaccharides to improve the stability of rice glutelin emulsions: Impact of polysaccharide type, pH, salt, and temperature. *Food Hydrocolloids, 64*(3), 112–122. https://doi.org/10.1016/j.foodhyd.2016.11.005

Xue, S., Qian, C., Yuan, H., Xu, X., & Zhou, G. (2018). High-pressure effects on myosin in relation to heat gelation: a micro-perspective study. *Food Hydrocolloids, 84*(11), 219–228. https://doi.org/10.1016/j.foodhyd.2018.06.014

Xue, S., Wang, H., Yang, H., Yu, X., Bai, Y., Tendu, A., et al. (2017). Effects of high-pressure treatments on water characteristics and juiciness of rabbit meat sausages: Role of microstructure and chemical interactions. *Innovative Food Science and Emerging Technologies, 41*(6), 150–159. https://doi.org/10.1016/j.ifset.2017.03.006

Yang, H., Han, M., Yun, B., Han, M., & Zhou, G. (2015). High pressure processing alters water distribution enabling the production of reduced-fat and reduced-salt pork sausages. *Meat Science, 102*(4), 69–78. https://doi.org/10.1016/j.meatsci.2014.10.010

Ye, T., Dai, H., Lin, L., & Lu, J. (2019). Employment of κ-carrageenan and high pressure processing for quality improvement of reduced NaCl surimi gels. *Journal of Food Processing and Preservation, 43*(9), Article e14074. https://doi.org/10.1111/jfpp.14074

Zhang, Z., Yang, Y., Tang, X., Chen, Y., & You, Y. (2015). Chemical forces and water holding capacity study of nanosized okara dietary fiber on gelation properties of silver carp surimiheat-induced myofibrillar protein gel as affected by high pressure.

Food Chemistry, 188(12), 111–118. https://doi.org/10.1016/j.foodchem.2015.04.129

Zhang, Z., Yang, Y., Tang, X., Chen, Y., & Yuan, Y. (2016). Chemical forces study of heat-induced myofibrillar protein gel as affected by partial substitution of NaCl with KCl, $MgCl_2$ and $CaCl_2$. *CyTA - Journal of Food, 14*(2), 1–9. https://doi.org/10.1080/19476337.2015.1091038

Zhang, Z., Yang, Y., Zhou, P., Zhang, X., & Wang, J. (2017). Effects of high pressure modification on conformation and gelation properties of myofibrillar protein. *Food Chemistry, 217*(2), 678–686. https://doi.org/10.1016/j.foodchem.2016.09.040

Zhu, Z., Lanier, T., & Farkas, B. E. (2015). High pressure effects on heat-induced gelation of threadfin bream (*Nemipterus spp.*) surimi. *Journal of Food Engineering, 146*, 23–27. https://doi.org/10.1016/j.jfoodeng.2014.08.021